

Total Coliform Modeling for McGrath Beach

by
C.P. Lai, Ph.D., P.E.
Los Angeles Regional Water Quality Control Board

1.0 Introduction

Water quality data collected indicate that portions of the McGrath Beach do not meet standards for total coliform. This report will describe the development of a model for use in identifying the pollutant sources in McGrath Beach Coastal Area and present the simulation results based on the data collected to help for the development of load reduction scenarios.

The mixing and dispersion of the wastewater discharge from a discharge point or structure like an outfall or a diffuser can be conceptually divided into two phases: (i) near field mixing, (ii) far field diffusion and buildup. The near field phenomenon occurs in a matter of minutes and within a region measured out to several hundred meters. The buildup in the far field occurs over days and weeks over distances beyond a few kilometers. The far field diffusion is in between these two scales, i.e., a time scale of hours to a few days and a distance scale of a few hundred meters to a few kilometers. For the near field, the mixing is dominated by discharge jet momentum. In this report, we will present the fundamentals of theory, description of the model, and simulation results for far field diffusion and buildup.

2.0 Theoretical Background of Water Quality Model (WQM)

Essentially, the far field model, as presented in the following, adopts the finite element model to provide more detailed analysis of pollutant's diffusion and buildup. It takes into account the complex geometry, such as intake structure, bay bathymetry and other environmental factors. In other words, the vertically integrated 2-D model considers the depth-wise variation in an average sense. Variations in the flow field in both the space and time are considered and included in the model. Given the design discharge layout and its environmental conditions, the model can be more readily applied to the detailed far field analysis for verification purposes.

2.1 Model Description

The numerical simulation is performed based on the WQM model first developed by Lee et al. (1985) for Fox River and Green Bay in Wisconsin and was modified by Environmental and Ocean Technology, Inc. (E.O. Tech) in 1989.

Based on the conservations of mass, momentum, and energy, the physical processes of water flow and material transport in a water body can be described by a set of partial differential equations. In general, three dimensional formulations are necessary to fully depict the complicated flow and transport phenomena. However, for riverine and coastal areas where the water depth is shallow, the flow variation with depth is not significant; water movement is mainly horizontal; vertical pressure distribution is effectively

hydrostatic; and water mixture is relatively homogeneous. Hence, the governing equations can be simplified by vertically averaged procedures and result in a set of two-dimensional equations. This is the approach adopted in deriving the fundamental equations for the model used in this study.

The numerical models are developed by using Galerkin's finite element method to solve the two-dimensional shallow water equations. Linear triangular shape function is used in the model. The detailed expression of this shape function can be found in Zienkiewicz (1977). A modified leapfrog scheme with mass lumping is employed for time integration (Lynch 1979).

Based on the assumption of constant water density, the equations governing the flow are uncoupled from those controlling the water quality distributions, and can be solved independently. Therefore, the simulation of the far field diffusion involves a two-step procedure: first, the hydrodynamic simulation is used to calculate the tide-induced currents and water elevations; second, the water quality simulation is applied to estimate the water quality distributions resulting from pollutant discharge based on the results of hydrodynamic simulation.

The basic formulations and the numerical techniques are explained in the following sections. Detailed simulation procedures such as model setup and verification are also included.

2.2 Governing Equations

The governing equations for hydrodynamic simulation are the continuity and momentum equations. For two-dimensional case, the governing equations are as follows:

$$\frac{\partial H}{\partial t} + \frac{\partial(Hu)}{\partial x} + \frac{\partial(Hv)}{\partial y} = 0 \quad (1)$$

$$\frac{\partial u}{\partial t} + u \frac{\partial u}{\partial x} + v \frac{\partial u}{\partial y} + g \frac{\partial \eta}{\partial x} - f v + \frac{\tau_x^b}{H} - \frac{\Psi_x}{H} - \frac{1}{H} \left[\frac{\partial}{\partial x} (H \varepsilon_x \frac{\partial u}{\partial x}) + \frac{\partial}{\partial y} (H \varepsilon_x \frac{\partial u}{\partial y}) \right] = 0 \quad (2)$$

$$\frac{\partial v}{\partial t} + u \frac{\partial v}{\partial x} + v \frac{\partial v}{\partial y} + g \frac{\partial \eta}{\partial y} + f u + \frac{\tau_y^b}{H} - \frac{\Psi_y}{H} - \frac{1}{H} \left[\frac{\partial}{\partial x} (H \varepsilon_y \frac{\partial v}{\partial x}) + \frac{\partial}{\partial y} (H \varepsilon_y \frac{\partial v}{\partial y}) \right] = 0 \quad (3)$$

In the above equations, all the dependent variables are vertically averaged quantities. Variable u and v are the velocity components in x and y directions, x direction is in the east and y direction is in the north; t the time; H the water elevation, f the Coriolis parameter; η the height of free water surface above the mean water level; τ^b the bottom shear stress; Ψ the surface shear stress; and ε the eddy viscosity.

The equation governing the distribution of water quality in water is the advective-diffusion equation based on the energy conservation as follows (for two-dimensional case):

$$\frac{\partial Q}{\partial t} + V \bullet \nabla Q - \frac{1}{H} \nabla \bullet (HK_c \bullet \nabla Q) + S_c + G_c = 0 \quad (4)$$

where Q is the concentration of water quality in the water body, V is the velocity vector in the flow field, K_c the diffusion-dispersion coefficient tensor, S_c the source/sink and the growth/decay of each water quality constituent, G_c the kinetic reaction of each water quality constituent that represents all important chemical and biological kinetic reactions involving the mass balance of substance. This interaction and mutual dependency are imbedded in the formulation of the source and sink and the kinetic reaction term which may involve a substance other than itself in the equation.

2.3 Principal Assumptions

The principal assumptions adopted in deriving the governing equations and numerical models are summarized as follows:

- (1) The density of water is constant.
- (2) The pressure in the water is hydrostatic.
- (3) The vertical distribution coefficients of the velocity components are equal and constant throughout the simulation domain.
- (4) The shear stresses from the vertical velocity component are neglected.
- (5) Only the gravity and Coriolis forces are considered.
- (6) The bottom shear stress is calculated according to the following equation (Dronkers, 1964):

$$\tau_b = \frac{gn^2|V|}{H^{\frac{4}{3}}}$$

where n is Manning's roughness coefficient.

- (7) The surface shear stress is correlated to wind speed, and is estimated by the following equation:

$$\varphi = \frac{C_d \rho_a V_w |V_w|}{\rho}$$

where ρ_a and ρ are the densities of air and water respectively, V_w the wind velocity vector at 10 m above the water surface, and C_d the wind drag coefficient.

2.4 Initial and Boundary Conditions

2.4.1. Hydrodynamic Simulation

For initial conditions, velocities u , v (x and y components) and water elevations have to be specified for every point in the model region. The model may be started from either a cold condition or a prestarting function. For the case of cold start, velocities at all the

nodal points are set to be zero and the water elevations are level. The prestarting function provided by this model is as $H_0 = H_1[0.5 - 0.5 \cos(\omega t)]$, in which ω is equal to $2\pi/T_p$ (T_p is the period of prestarting determined by the user), t the elapsed time from the beginning, H_1 the initial water level, H_0 the water level specified at the open boundaries during the prestarting period.

Two types of boundary conditions can be prescribed as functions of time at each boundary node: velocities and water elevations. In general, water elevations are specified at open boundaries according to the changes of tidal amplitudes. At solid boundaries, the normal velocity component is often set to zero.

2.4.2 Water Quality Simulation

The model requires a proper initial condition, which will specify water quality at every nodal point in the simulation domain at time zero. Usually, the model starts with a uniform water quality distribution with a typical value for the modeling area.

Two types of boundary conditions can be chosen for the convective transport equations for water quality pollutant discharge:

- (1) prescribed water quality concentration
- (2) prescribed dispersive flux perpendicular to the tangent at the boundary node

In general, normal dispersive flux is set as zero at land boundaries, while it is equal to the strength of flux at source or sink points.

The imposition of boundary conditions at the open boundaries is a difficult task for any numerical model that attempts to estimate the solution for the advective diffusion equation in a restricted area. No generally valid method is available for prescribing such a boundary condition. One method is to impose a no-flux boundary condition and assume the boundaries to be sufficiently far away so that within the times of simulation, that there is no effect from the boundaries. Sometimes it is possible to locate open boundaries of simulated regions at some actual physically meaningful boundaries (such as at the edge of major ocean current systems) and then utilize a Dirichlet boundary condition. If the water quality concentration at the boundaries is known or can be estimated using other methods, a type (1) boundary condition can also be used to specify fixed values at open boundary points.

2.5 Model Verification

Both the hydrodynamic and water quality models have been verified for the cases amenable to analytical solutions (Wang, 1975). In addition, these two models have been tested through the simulation of the Fox River and Green Bay system and proved to be a suitable numerical tool for studying the transport phenomena in the coastal areas (Lee et al., 1985). Other studies also show that they can be successfully applied for the far field simulations (E.O.Tech., 1991 and 1998).

3.0 Model Development

3.1 Hydrodynamic Model Set-up

3.1.1 Finite Element Grid and Modeling Parameters

A finite element grid layout was set up for hydrodynamic and water quality simulations for the total coliform discharges from McGrath Beach Coastal Area. This grid (Figure 3.1) covers an alongshore distance of about 14 kilometers (km) and extends offshore about 7 km. This basin is constructed by describing the geometry of the area with triangular elements. The total number of elements is 3726, and that of nodal points is 1994. The linear dimension of the elements is from 100 to 300 meters (m).¹ The mesh size of the grid is chosen in such a way as to provide a satisfactory resolution of the water elevation and water quality distribution in the vicinity of McGrath Beach Area. The bathymetry topography used is digitized based on available charts (NOAA nautical chart No.18720, 7/29/2000).

The values of Manning n used in the hydrodynamic simulation to calculate the bottom friction is from 0.03 at the nearshore area down to 0.015 at the offshore area. These values are based on the calibrated flow speed. The computation time step Δt is 5 sec for the computational grid. Internal stresses and wind induced surface stresses are of less importance, so their effects were not simulated. The computation area is so small that wind induced current velocity will not be vary significantly and the rip current is considered only for the deeper water depth, usually greater than 20 meters deep.

3.1.2 Boundary Conditions

The simulations adopt a cold start, which means that the water elevations are level and velocities are zero everywhere in the basin.

At the solid boundaries, zero normal flow is assumed as corresponding boundary condition. In addition, each grid has three open boundaries, all of which are implemented as water-level boundaries, i.e., water elevations are specified at boundary nodal points. The predicted tide data² (National Oceanographic Data Center, 2001) at Ventura are used as the basis for the interpolation of water elevations along the open boundaries (Figure 3.2).

3.2 Water Quality Model Set-up

3.2.1 Water Quality Simulation Parameters

The computation time step Δt used in water quality simulation is 180 sec.

The dispersion coefficients, D_x , D_y are among the controlling factors in determining the solutions of the advective transport equation. They can also affect the stability of the numerical schemes used to solve this equation. It is very important to take into considerations their physical meanings and numerical implications when values are

¹ This was used over a 3-D model, as a 3-D model does not necessarily produce good results, especially for the shallow water area without a stratified flow situation.

² For tide data, there are only spring, mean and neap tide conditions. In this study, we use the mean tide condition.

selected for the modeling. In general, the dispersion coefficients vary locally according to velocity distribution, water depth, bottom roughness, etc. For this model, through extensive testing and calibration, the following equations are found to be suitable for the estimation of the dispersion coefficients (Lee 1986):

$$D_x = C_x \sqrt{2A} \sqrt{gH}$$

$$D_y = C_y \sqrt{2A} \sqrt{gH}$$

where A is the area of individual elements in the grid system, g the gravitational acceleration constant, H local water level, C_x and C_y dimensionless constants determined by numerical experiments in model calibration, and founded to be between 0.002 and 0.005 based on previous experience (Lee 1986).

The sources of total coliform in this study are the total coliform discharge from Santa Clara River, McGrath Lake, and Mandalay Generating Station. The average wet weather flow rates of three potential sources are 213, 10.1, and 143 MGD, respectively. A single die-off value is used as the first order decay coefficient for the whole computation domain. The die-off rate for total coliform in seawater is 0.7 to 3.0 per day according to the *Protocol for Developing Pathogen TMDLs* (2001). In this study, we use 0.8 per day for total coliform in the model.

3.2.2 Water Quality Boundary Conditions

Total coliform simulation is based on the finite element system described by the computational grid. Computation starts with a uniform zero concentration throughout the simulation basin. At the land boundary nodes, perpendicular flux is assumed to be zero.

4.0 Simulation Results

4.1 Hydrodynamic Simulation Results

Figure 4.1 shows the computed tidal water levels at the Mandalay Generating Station. This figure illustrates that the simulated tidal ranges are between 1.6 to 1.8 m, which are consistent with the mean tidal range of 1.7 m observed in the field.

The calculated time series of current speed and direction at the Mandalay Generating Station are also presented in the Figure 4.1. The magnitude of currents observed at the Mandalay Generating Station is between 3 to 5 cm/sec most of the time, with a median value around 4 cm/sec. The simulated current speeds are within this range with a smaller median of about 3.2 cm/sec. Concerning the direction of currents, the results show two dominant directions: northwest (corresponding to 135° in Figure 4.1), and between southeast and southwest (corresponding to 300°). Our simulation results agree well with the field observation. Similarly, the calculated tidal water levels and current speed at the McGrath Lake outfall and the Santa Clara River are presented in Figures 4.2 and 4.3 respectively. The directions change significantly for the Santa Clara River. This is because the Santa Clara River is measured at its mouth and therefore it is affected by boundary. The McGrath Lake outfall and Mandalay Generating Station are not measured at their respective boundaries, and therefore are not affected.

Previous studies also show that the flow in the vicinity of the McGrath Beach site is mainly tide-induced. Flow pattern is generally parallel to the shoreline. Flow direction is toward the northwest during the flood tide, and toward southeast during ebb tide. Figures 4.4 to 4.5 present the simulated patterns of tide-induced currents at different tidal phases in the study area. It can be seen that the simulation results are consistent with the general description of the local flow field.

4.2 Validation of the Model

To further examine the model's ability to predict a real physical situation, a subsequent testing of a pre-calibrated model to additional field data is required. This process is usually called *validation of the model*. In this study, the field data collected at Santa Clara River, McGrath Lake, and Mandalay Generating Station were used for model validation. The data used for validation are summarized in Table 4.1. The results of model validation at the Santa Clara River, the McGrath Lake outfall, and the Mandalay Generating Station are presented in Figure 4.6 and 4.7, respectively. It can be seen that the results of the model and field results are well correlated, specially for Santa Clara River.

4.3 Total Coliform Simulation Results

In water quality simulation, three different input conditions for dry and wet weather situations are used for evaluating the discharges from Santa Clara River, McGrath Lake, and Mandalay Generating Station. These three typical discharge conditions are based on the geometric mean, 80 percentile and maximum of historical effluent data collected during the period of 1984 to 2001 for Santa Clara River and that of 2002 for McGrath Lake and Mandalay Generating Station, which are shown in the Table 4.2 for dry weather and Table 4.3 for wet weather.

During water quality simulations, sufficient simulation time was used in each run to assure quasi steady-state conditions. Figure 4.8 shows typical time series of concentration rise of total coliform at Mandalay Generating Station in the simulation basin. It can be seen from Figure 4.8 that the solutions reach steady state after about 20 hours to 30 hours, with a periodic rise and fall. Ten days were used in this study to provide the results on total coliform concentration distributions. This Figure also illustrates that total coliform concentration rises change within a tidal cycle after reaching steady state. These results are the steady state results with variation due to the effect of tidal influence.

Figure 4.9 is an example illustrating the maximum total coliform concentration distribution for the whole computation domain the geometric mean concentration of the discharge from all three potential locations, during dry weather. Since this figure covers a large area, it does not give enough resolution for the surrounding area of the discharge points. In order to provide better spatial resolutions, all the other results are presented for a smaller area.

Figures 4.10 to 4.13 are the spatial distributions of maximum total coliform concentrations as simulated by the WQM model for the discharges of Santa Clara River, McGrath Lake, and Mandalay Generating Station. These figures consider the geometric

mean (Figures 4.10 and 4.12) and maximum (Figures 4.11 and 4.13) discharge conditions in dry (Figures 4.10 and 4.11) and wet (Figures 4.12 and 4.13) weather situations respectively. In all the figures, the concentration of total coliform are expressed in MPN/100 mL. From these figures, the areas affected by each discharge plume can be identified. Most of the plumes are toward the southeast after a repeated tidal effect simulated for 10 days. During dry weather, the highest simulated concentrations are at the discharge of the Mandalay GS, which also produces the largest plume due to the high discharge flowrate (Figure 4.11). However, when the geometric mean of the outfall concentrations is considered, the area near the discharge of McGrath Lake has the highest concentrations (Figure 4.10). Note that only a small area is affected along the two miles of beach front. During wet weather, the largest impact is from the SCR estuary when it breaches at maximum total coliform concentration, which generates a plume of coliform. (Figure 4.13). When the geometric mean concentrations in the outfalls are considered, the highest simulated concentrations at the beach occur near McGrath Lake (Figure 4.12)

Figure 4.14 and 4.15 show the results of the concentration rise versus the distance along McGrath Beach to represent the direct effects on the beach due to these discharge scenarios. In Figures 4.14 and 4.15, the reference point of distance is situated in the Oxnard State Beach and the distance of three discharge points are 5130 m, 6860 m, and 8680 m. Based on these figures, we can see that total coliform concentrations greater than 1000 MPN/100 mL in McGrath Beach are due to the Mandalay Generating Station, McGrath Lake, and Santa Clara River during dry weather conditions if the maximum or 80 percentile concentrations in the outfall are considered. During wet weather conditions the maximum total coliform concentrations are near the Santa Clara River estuary and the McGrath Lake outlet if the maximum outfall concentrations are considered, and near the McGrath Lake outlet if the 80 percentile outfall concentrations are considered.

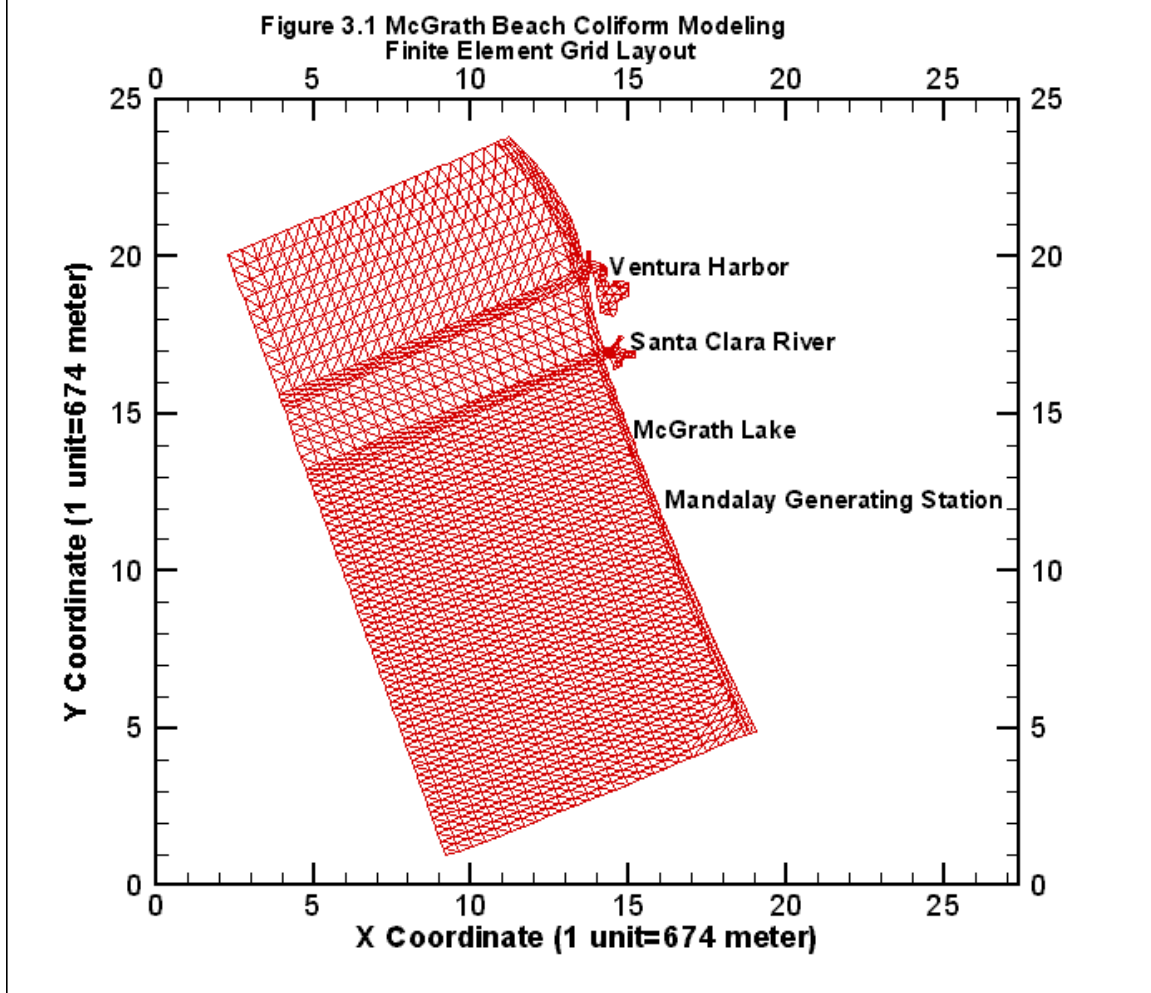
5.0 Concluding Remarks

The water quality data collected from the field indicated that the McGrath Beach do not meet the water quality standard of total coliform. This report utilizes an accepted water quality model to simulate total coliform in the McGrath Beach Coastal Area. The results of the simulations show that the impairment of water quality in McGrath Beach are primarily due to the effluent discharge from Mandalay Generating Station and McGrath Lake during dry weather and Santa Clara River and McGrath Lake during wet weather. These results are based on the effluent discharge data collected and consider tidal effect only.

6.0 References

1. Environmental and Ocean Technology, Inc. Numerical Simulation of Waste Discharge from the Eureka Paper Mill in Eureka Coastal Area, California, 1991.
2. Environmental and Ocean Technology, Inc. Water Quality Modeling in Los Angeles and Long Beach Harbors, California, 1998.
3. McGrath Lake Watershed Action Committee, Personal Communication, 2001.

4. King I.P. and Norton W.R. (1978), Recent Application of RMA's Finite Element Models for Two Dimensional Hydrodynamic and Water Quality, Finite Element in Water Resources.
5. Lee, K.K. and Chen, C.L. A Dynamic Water Quality Simulation Model for a Freshwater Estuary and Riverine System, International Conference on Water Quality Modeling in the Inland Natural Environment, Bournemouth, England, June, 1986.
6. Lee, K.K. and Chen, C.L. A Hydrodynamic and Water Quality Model for the Fox River and Green Bay, Sea Grant Project R/GB-19, University of Wisconsin, Milwaukee, Wisconsin, 1985.
7. Lynch, D.R. and W.G. Gray, A Wave Equation Model for Finite Element Tidal Computations, Computers and Fluids, Vol.7, No.3, pp207-228, 1979.
8. MBC Applied Environmental Sciences. National Pollutant Discharge Elimination system 2000 Receiving Water Monitoring Report Reliant Energy Mandalay Generating Station, Ventura, California, 2000.
9. U.S. Environmental Protection Agency, Protocol for Developing Pathogen TMDL, EPA 841-R-00-002, January 2001.
10. Wang, J.D. and J.J. Connor. Mathematical Modeling of Near Coastal Circulation, Report No. 200, Ralph M. Parsons Laboratory, Massachusetts Institute of Technology, Cambridge, Mass., p271, 1975.
11. Zienkiewicz, O.C. The Finite Element Method in Engineering Science, McGraw-Hill, London, 1977.



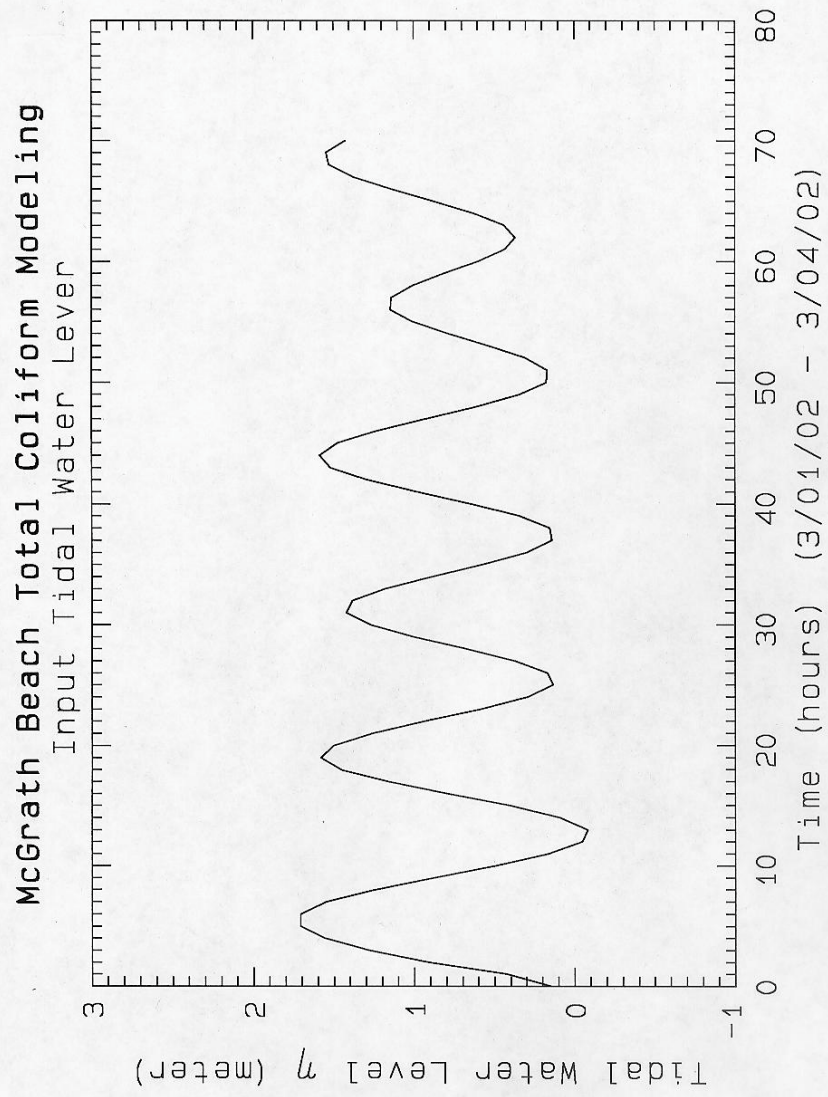


Figure 3.2 Input Tidal Water Level in McGrath Beach Coastal Area.

Table 4.1 Validation Data for
McGrath Beach Total Coliform Modeling

Validation Data for Santa Clara River												
Month	Day	Year	R1	R2	R3	R4	L5	R5	R6	R7	R8	R9 Q(cfs)
6	10	86	16000	24001	24001	24001	16000	2401	2401	920	540	34
11	18	86	24001	24001	24001	24001	24001	2401	2401	2401	2401	48.5
7	19	88	2200	1100	16000	9200	1100	33	240	350	23	5.92
6	9	92	9200	2400	16000	3500	24000	130	350	170	350	9.69
9	21	93	1400	1400	16000	3500	24001	350	540	170	79	12.93
11	23	93	790		24001	1700	24001	240	2401	540	49	29.73
7	5	94	350	24001	24001	350	5400	8	2401	17	27	24.13
11	7	95	5400	3500	9200	5400	3500	240	350	280	170	7.5
6	18	96	2400	2400	2400	700	24001	49	540	70	22	96.94
7	29	97	2400	9200	9200	9200	1	5	220	4	5	10.5
6	16	98	5400	490	1700	790	490	240	920	79	240	193.88
			R3 Q(cfs)	Q(cms)	R*Q	R6 (sampling results)	R6*(calculated)					
			Index			1	2401	2505	(6/10/86)			
1	24001	34	0.96288	1.99684E+13								
2	24001	48.5	1.37352	2.84843E+13			2401		(7/19/88)			
3	16000	5.92	0.167654	2.3178E+12			3	240	291	(6/09/92)		
4	16000	9.69	0.274421	3.79383E+12			4	350	478	(9/21/93)		
5	16000	12.93	0.366178	5.06235E+12			5	540	637	(11/23/93)		
6	24001	29.73	0.841954	1.74606E+13			2	2401	2193	(11/07/95)		
7	24001	24.13	0.683362	1.41717E+13			2401		(6/18/96)			
8	9200	7.5	0.2124	1.68843E+12			6	350	211	(7/29/97)		
9	2400	96.94	2.745341	5.69309E+12			8	540	713	(6/16/98)		
10	9200	10.5	0.29736	2.3638E+12			7	220	294			
11	1700	193.9	5.490682	8.06521E+12			9	920	1011			
Validation Data for McGrath Lake												
C(MPN/100 mL)												
1	16,000	4.23	0.12	1.70E+12		1700		1845	(4/02/02)			
2	1600	4.23	0.12	1.70E+11		500		185	(4/09/02)			
Validation Data for Mandalay Generating Station												
1	90	97.72	2.77	2.16E+11		2		35	(5/06/02)			
2	240	34.92	0.99	2.04E+11		130		31	(4/09/02)			

Table 4.2 McGrath Beach Input Data in Dry Weather (May-October)

[illegible]

Table 4.3 McGrath Beach Input Data In Wet Weather (November-April)

	Santa Clara River Flow Rate (cfs)	Santa Clara River Total Coliform (MPN/ 100 mL)**	McGrath Lake Flow Rate (MGD)	McGrath Lake Total Coliform (MPN/100 mL)	Date	Mandalay G.S. Flow Rate (MGD)	Mandalay G.S. Total Coliform (MPN/100 mL)	Date
November		2198	10.1	24192	11/8/99	130	230	11/?/?/01
December		420	10.1	24192	1/16/01	147	50	2/19/02
January		2704	10.1	19863	1/22/01	148		
February		663	10.1	17329	1/23/02	136		
March		941	10.1	24192	2/12/01	140		
April		1451	10.1	24192	2/26/01	159		
Sum(1984-2001) (cfs)	5930.57		60.6	24192	2/5/02	860		
Average (MGD)	212.98		10.1	19863	2/12/02	143.3333333		
Average (cms)	9.328524		0.44238	24192	2/20/02	6.278		
Average (cfs)	329.48006		15.6247	24192	2/26/02	221.7366667		
				24192	3/5/02			
				24192	3/6/01			
			Based on 7000 gallons/min	24192	3/12/01			
				24192	3/27/01			
				16000	4/2/02			
				1600	4/9/02			
				13000	4/24/02			
Geomean		1145.536782		18589.21037			107.2380529	
80 percentile		3500		24192			194	
Maximum		24000		24192			230	
Mass loading								
Geomean (org/day)		9.24×10^{12}		7.11×10^{12}			5.82×10^{11}	
80 percentile (org/day)		2.82×10^{13}		9.25×10^{12}			1.05×10^{12}	
Maximum (org/day)		1.93×10^{14}		9.25×10^{12}			1.25×10^{12}	
	$(X * 10^6 \text{ gal/day}) * (3.785 * 10^{-3} \text{ ml/gal}) * (Y \text{ organisms}/100 \text{ ml})$ $= (3.785 * 10^3 * X*Y) \text{ organisms/day}$							
** The concentrations listed here are the average of the month								

McGrath Beach Tidal Current Simulation

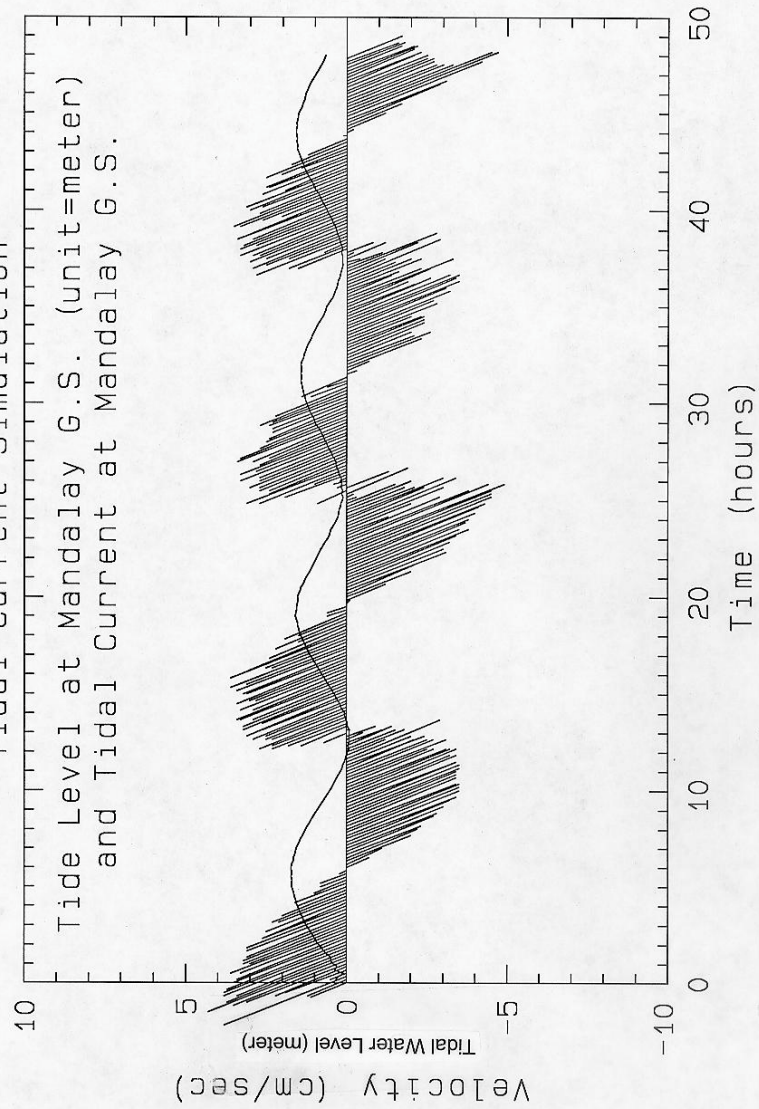


Figure 4.1 Calculated Tidal Water Levels and Currents at Mandalay Generating Station.

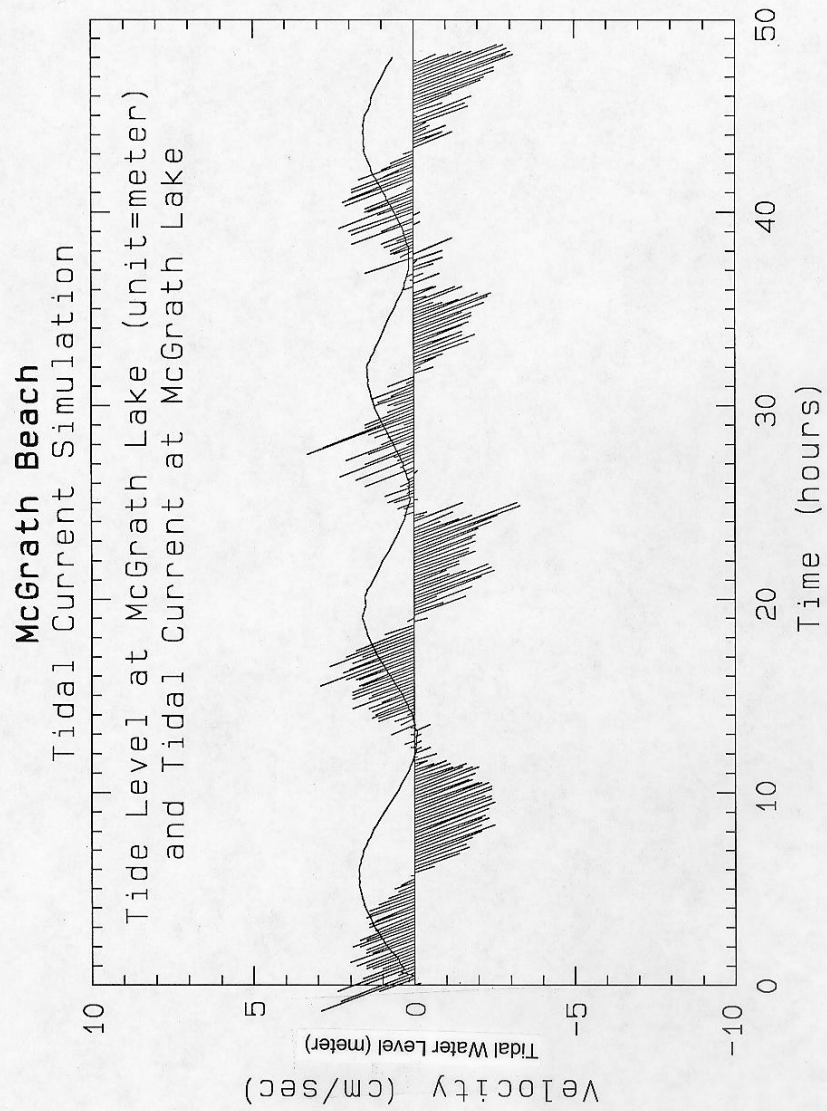


Figure 4.2 Calculated Tidal Water Levels and Currents at McGrath Lake.

McGrath Beach Tidal Current Simulation

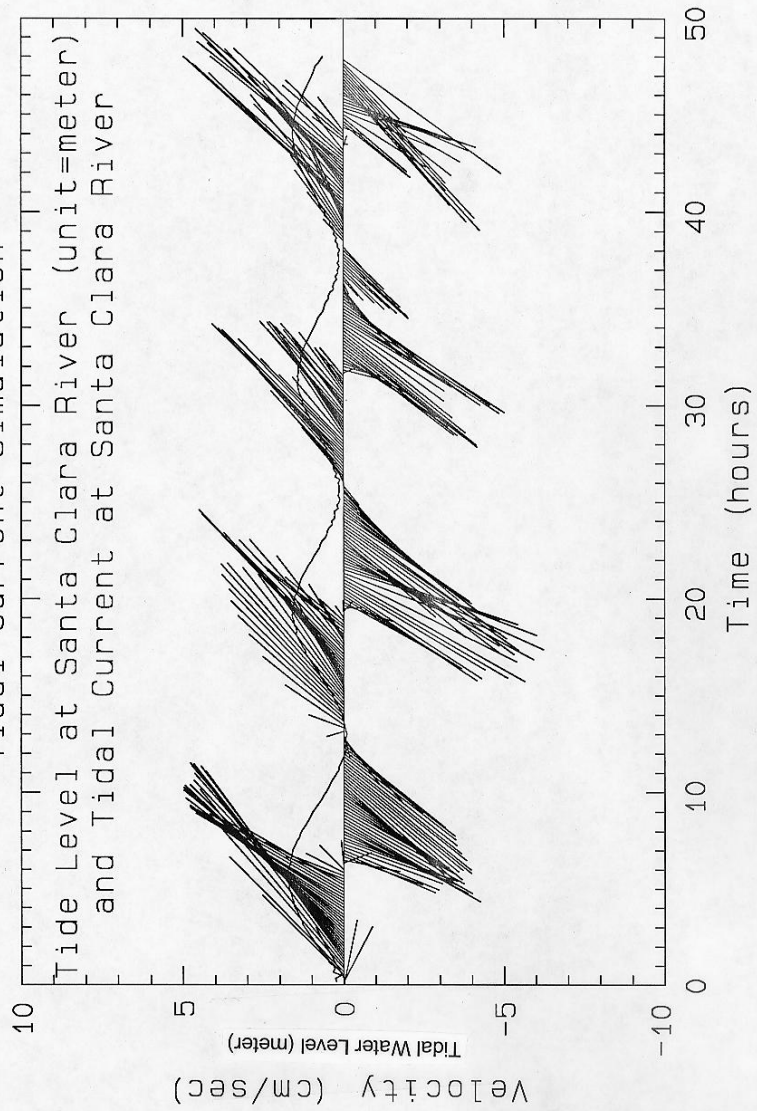
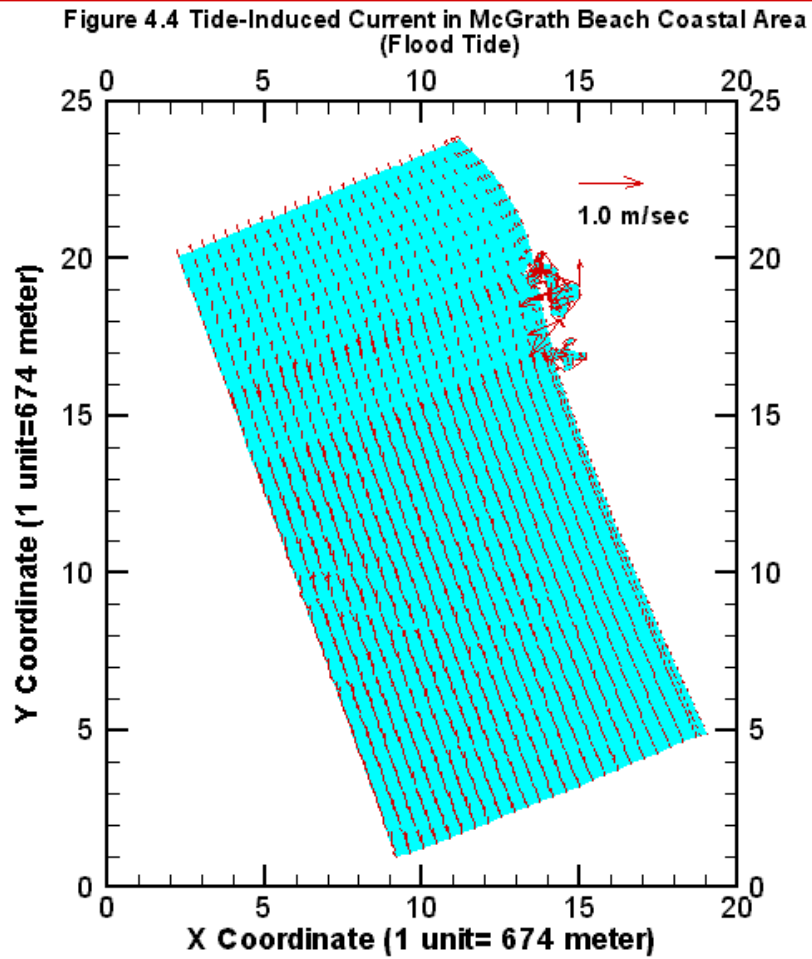
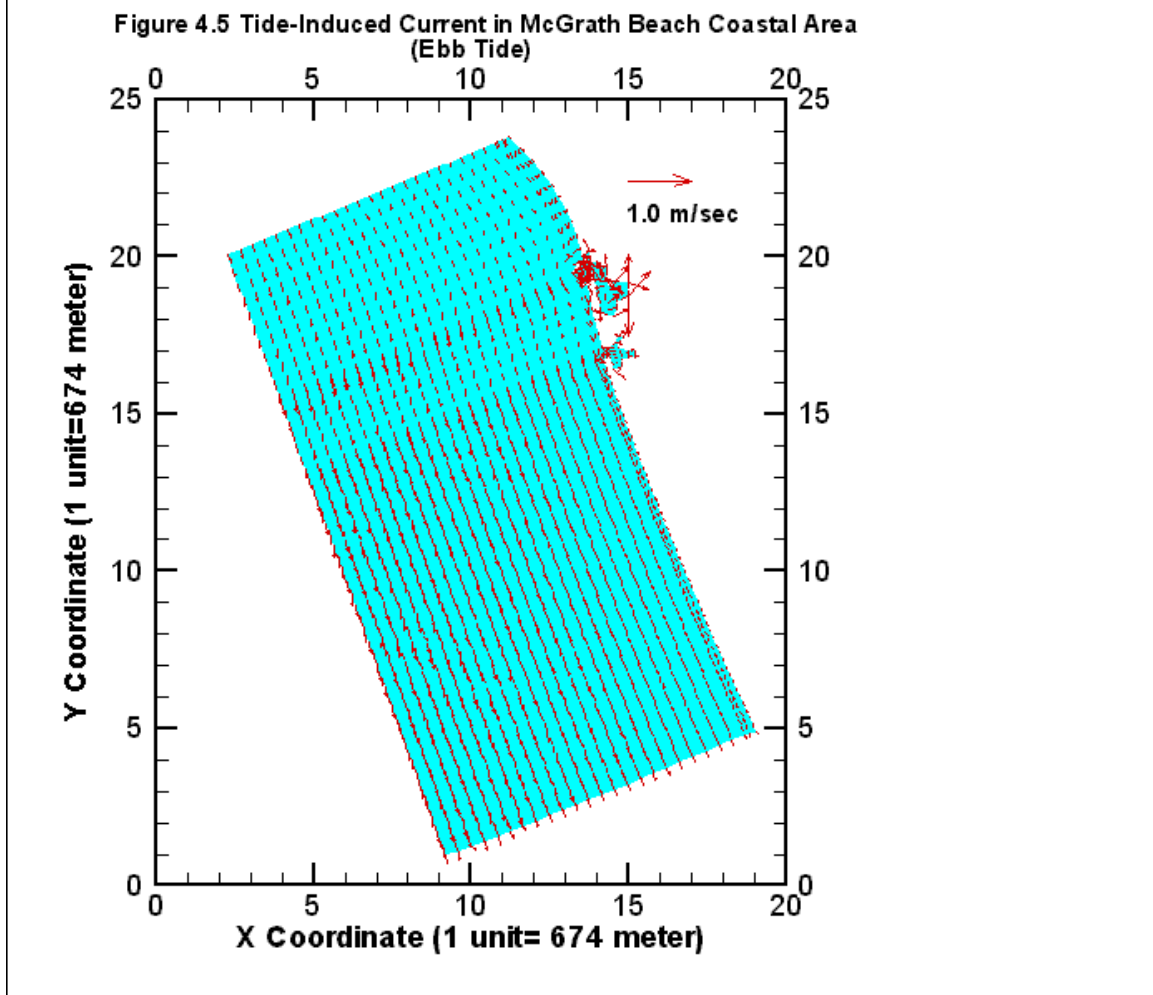


Figure 4.3 Calculated Tidal Water Levels and Currents at Santa Clara River.





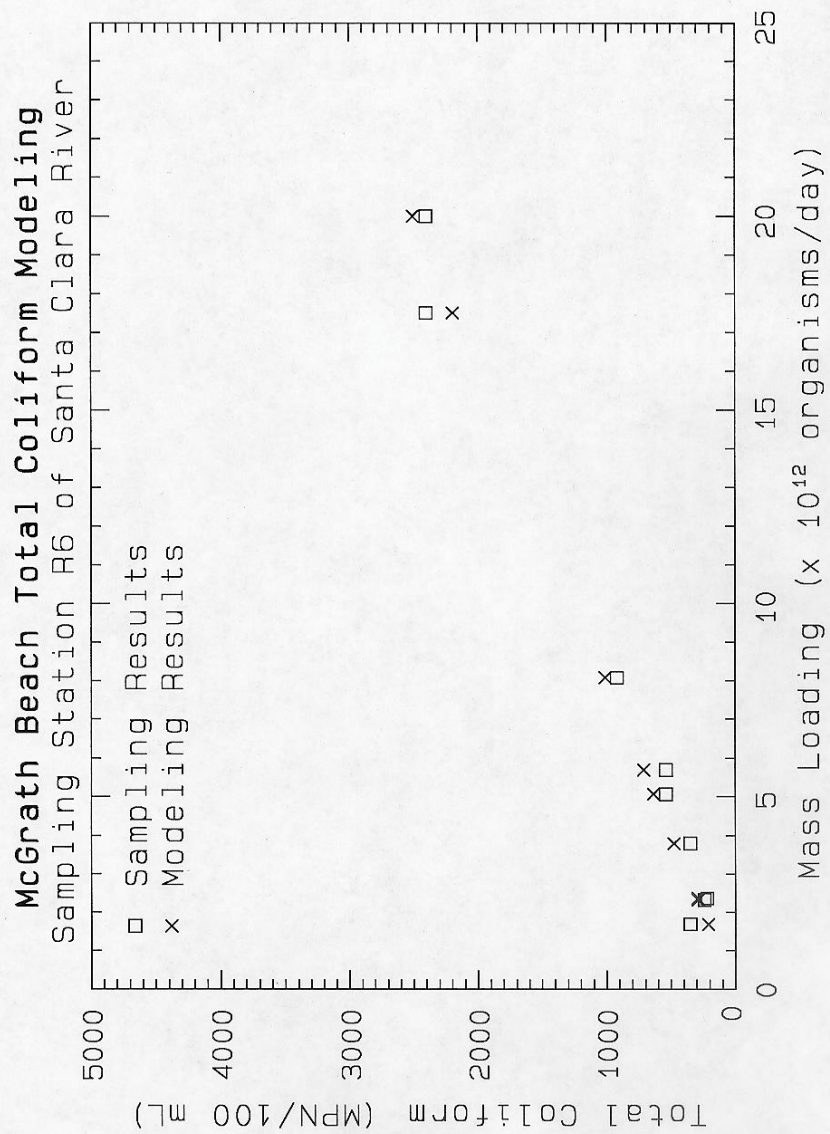


Figure 4.6 Comparison of Modeling Results and Sampling Results at Santa Clara River.

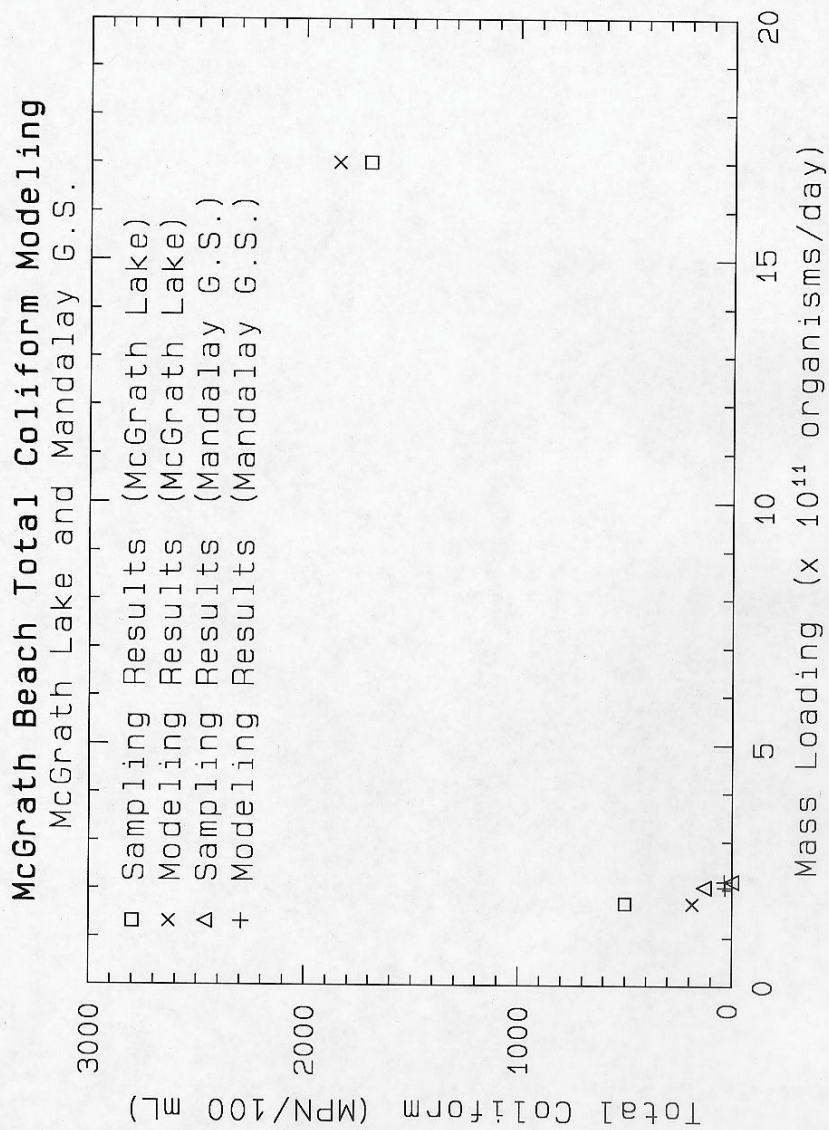


Figure 4.7 Comparison of Modeling Results and Sampling Results at McGrath Lake and Mandalay Generating Station.

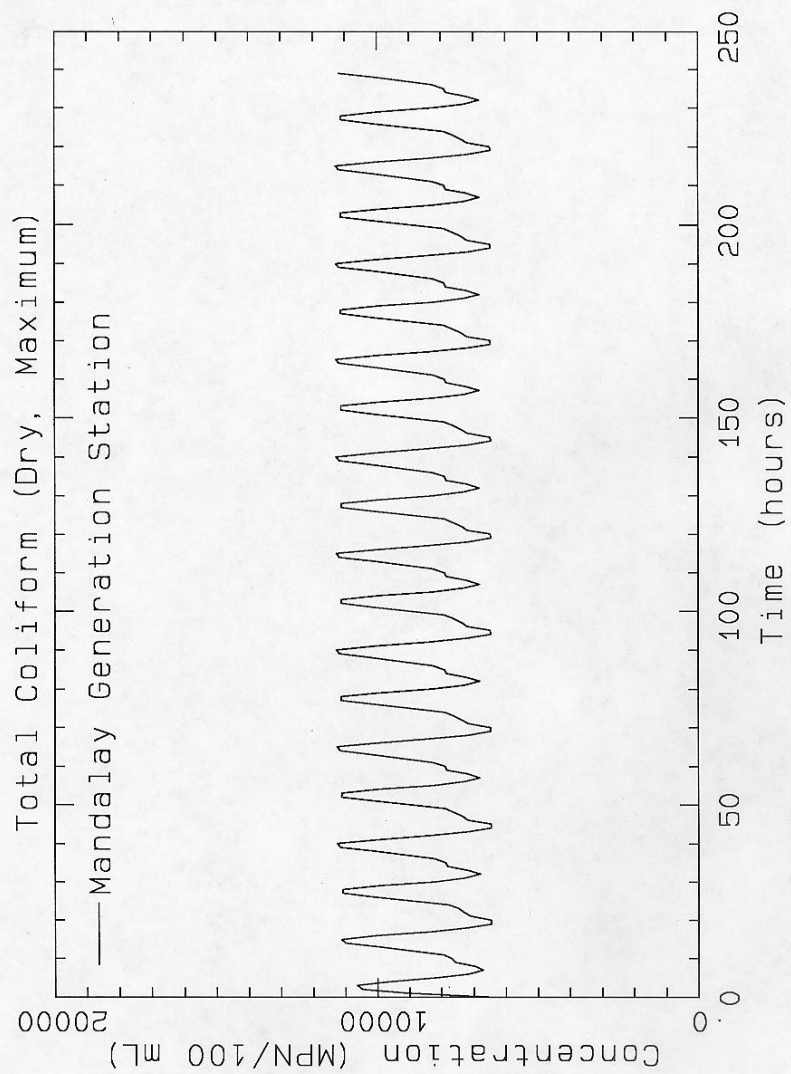
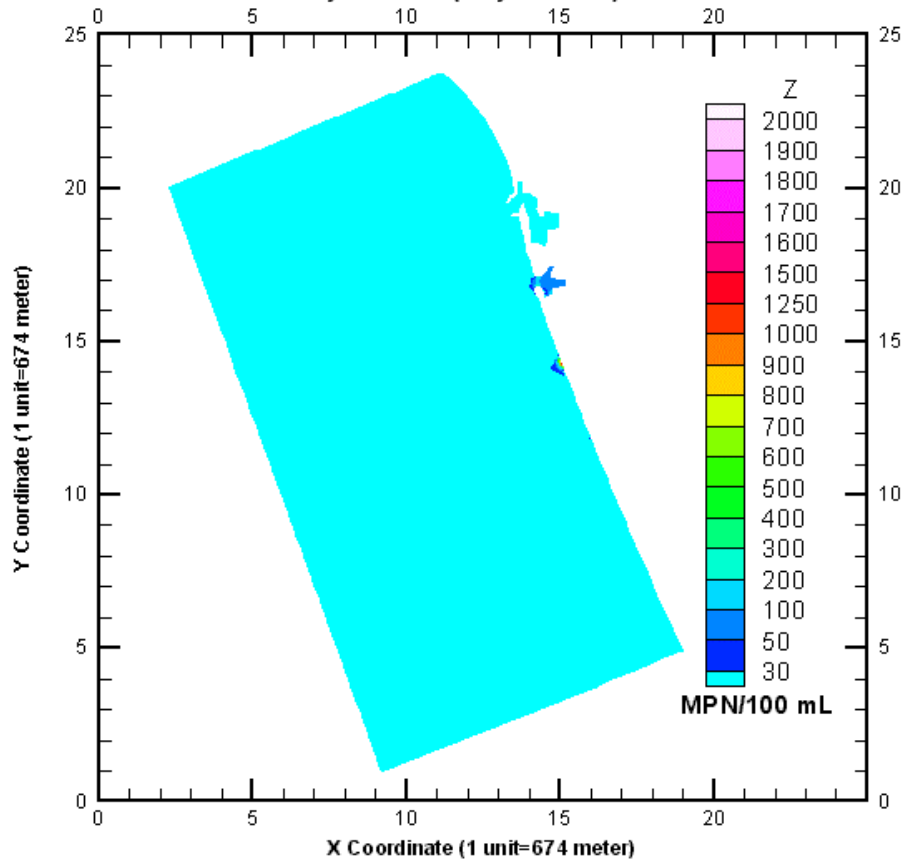
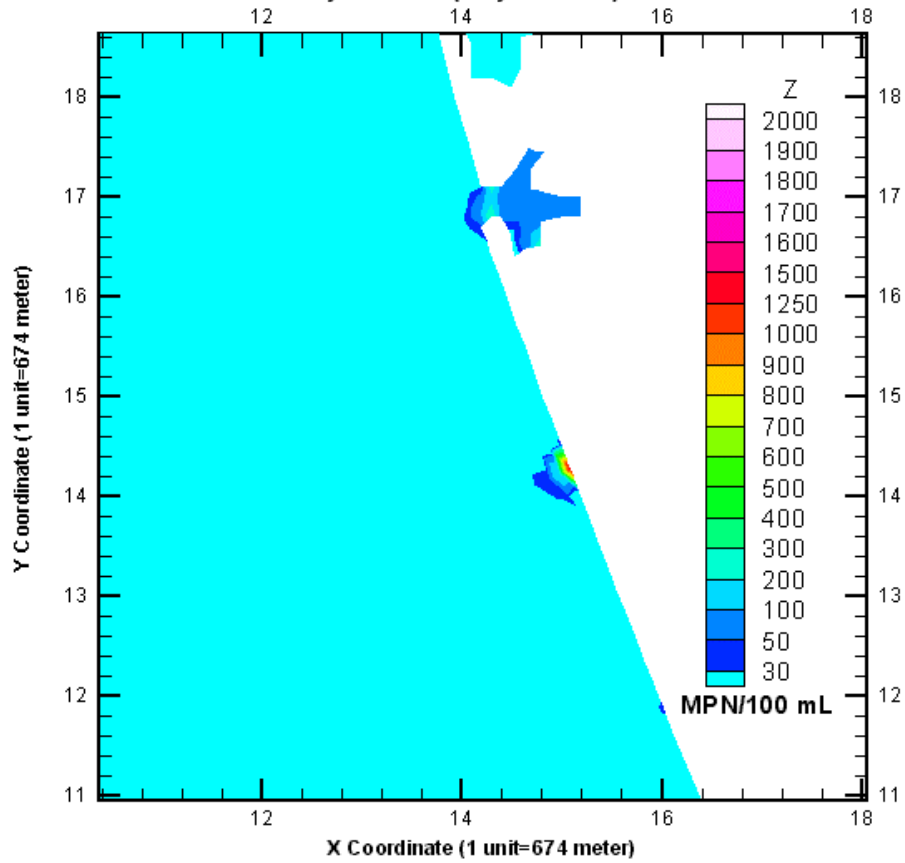


Figure 4.8 Calculated Time Series of Total Coliform Concentration Rises at Mandalay Generating Station.

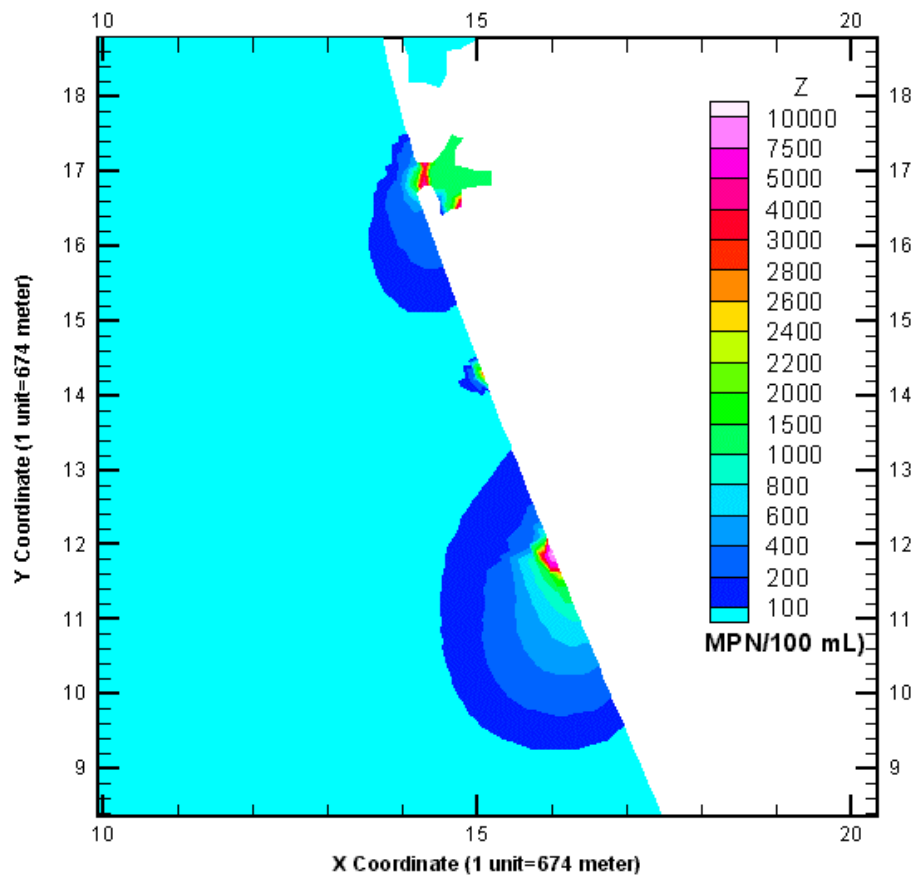
**Figure 4.9 McGrath Beach Total Coliform Modeling
Using Geometric Mean of Historical Effluent Data
in Dry Weather (May-October)**



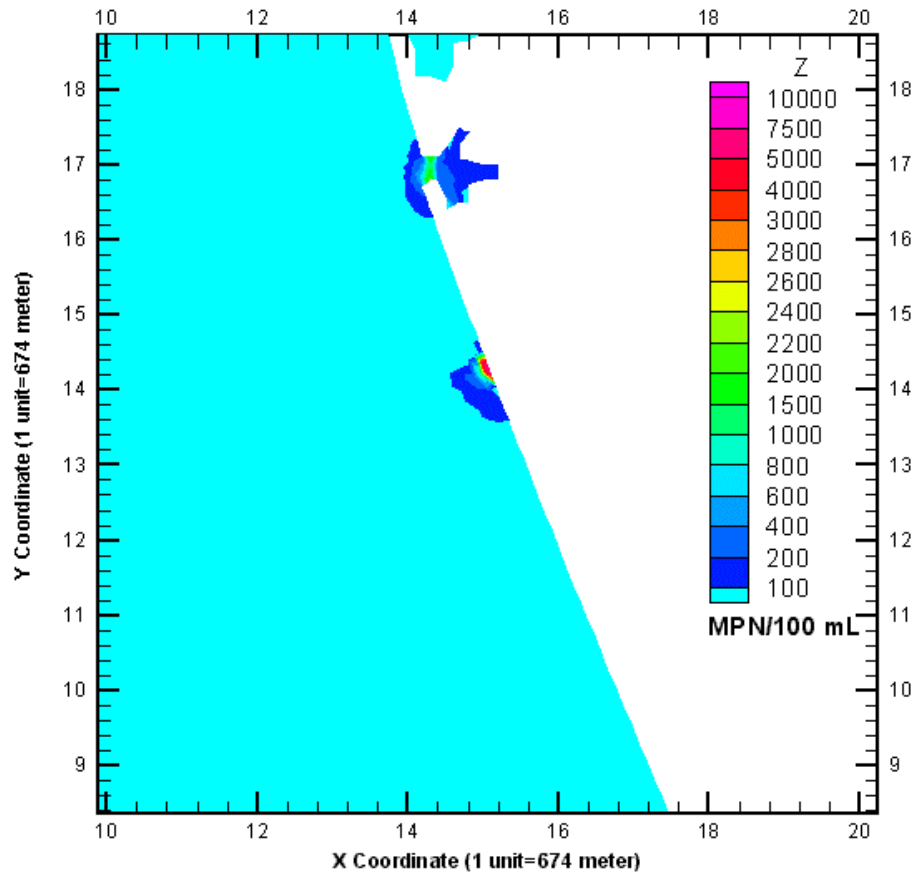
**Figure 4.10 McGrath Beach Total Coliform Modeling
Using Geometric Mean of Historical Effluent Data
in Dry Weather (May-October)**



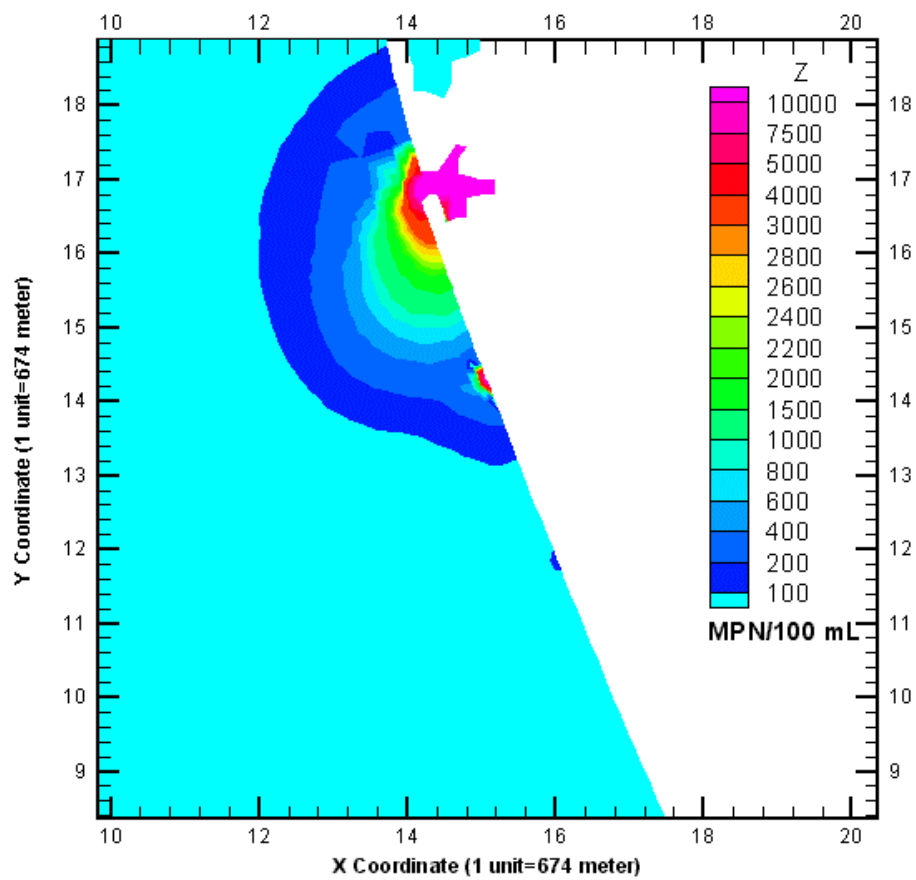
**Figure 4.11 McGrath Beach Total Coliform Modeling
Using Maximum of Historical Effluent Data
in Dry Weather (May-October)**



**Figure 4.12 McGrath Beach Total Coliform Modeling
Using Geometric Mean of Historical Effluent Data
in Wet Weather (November to April)**



**Figure 4.13 McGrath Beach Total Coliform Modeling
Using Maximum of Historical Effluent Data
in Wet Weather (November to April)**



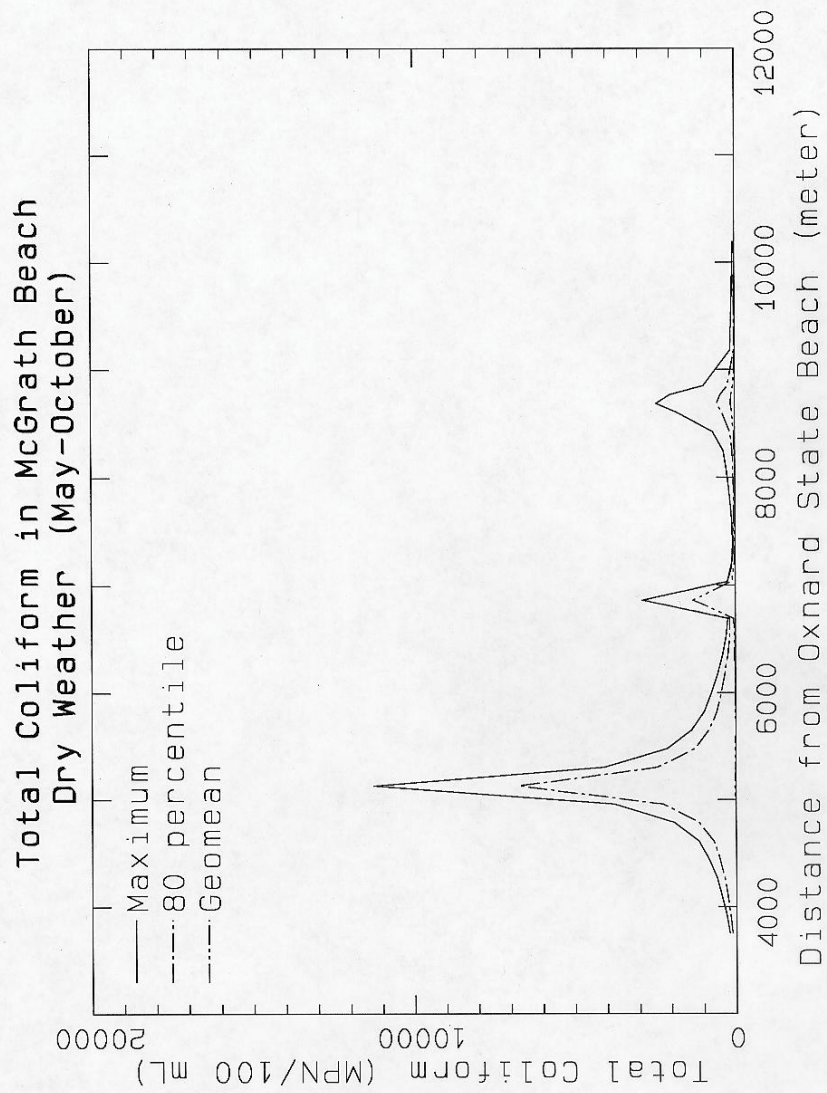


Figure 4.14 Modeling Results of Total Coliform Concentration Rises Along McGrath Beach in Dry Weather.

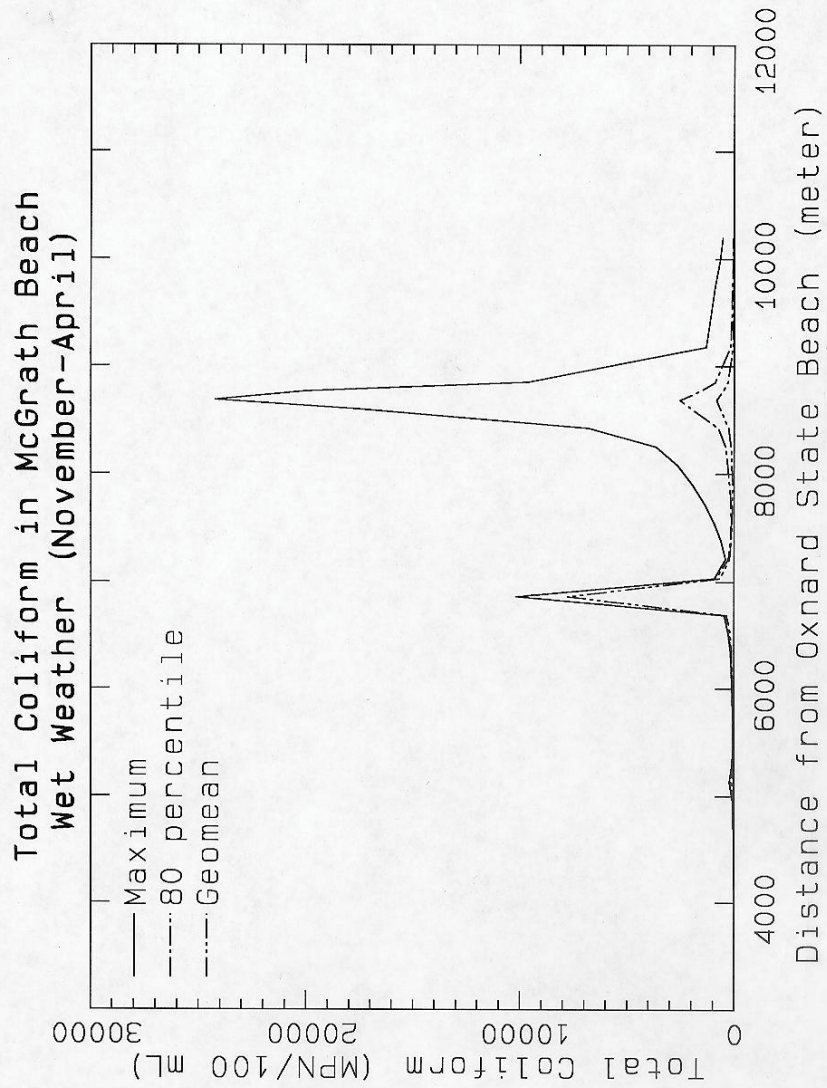


Figure 4.15 Modeling Results of Total Coliform Concentration Rises Along McGrath Beach in Wet Weather.